Optical constants of methyl-pentaphenylsilole by spectroscopic ellipsometry

H. J. Peng, Z. T. Liu, H. Y Chen, Y. L. Ho, B. Z. Tang,[a] M. Wong, H. C. Huang, and H. S. Kwok[b]
Center for Display Research Department of Electrical and Electronic Engineering, The Hong Kong University of Science and Technology, Clear Water Bay, Kowloon, Hong Kong

(Received 4 December 2001; accepted 13 August 2002)

The optical properties of 1-methyl-1,2,3,4,5-pentaphenylsilole thin films grown on silicon substrate were investigated using spectroscopic ellipsometry (SE). Accurate refractive index n and extinction coefficient k, in the wavelength range of 250 to 800 nm, were determined. Sellmeier equations, amorphous semiconductor model, and a three-oscillator classical Lorentz model were used to fit the data in different spectral ranges. A band gap of 2.78 eV and uv absorption peaks at 368 and 263 nm were derived from the SE spectrum. Additionally, the absorption spectra near the major band edges show optical properties similar to that of an amorphous semiconductor. © *2002 American Institute of Physics.* [DOI: 10.1063/1.1512312]

I. INTRODUCTION

Organic light-emitting diodes (OLEDs) have attracted a great deal of attention because of their great application potential and excellent properties such as high luminance, low power consumption, and full color capability.[1] OLEDs are also relatively easy to manufacture and package. The most commonly used emitter material is tris(8-hydroxyquinoline) aluminum (Alq_3) which can also act as an electron transport layer. Conventional undoped small-molecule OLED using Alq_3 can achieve a high external quantum efficiency η_{QE} of 1.5%.[2] Recently, We found a fluorescent organic emitter, 1-methyl-1,2,3,4,5-pentaphenylsilole (MPS), that can achieve a high η_{QE} of 8%.[3] However, much of the optical and electrical properties of this new compound are unknown. It is therefore the objective of this paper to measure the optical constants of this new material, including the refractive index n and the extinction coefficient k. These optical constants are needed for optimizing the design of this device, such as in microcavities, as well as in understanding properties such as external light coupling efficiency.[4,5]

In this study, n and k were measured using spectroscopic ellipsometry (SE). We found that it is possible to fit the optical dispersion of n and k using different models in different wavelength regions. The data were interpreted in terms of an absorption peak in the blue region and two secondary peaks in the uv. The absorption peak from SE corresponds well with the band gap of MPS, measured by absorption spectroscopy and cyclic voltammetry (CV). It was also found that the absorption spectra near the band edge could be well fitted by treating MPS as an amorphous semiconductor. Finally, we discuss the implication of our results on the photon extracting efficiency of the emitting devices.

[a]Department of Chemistry.
[b]Author to whom correspondence should be addressed; electronic mail: eekwok@ust.hk

II. SPECTROSCOPIC ELLIPSOMETRY

Spectroscopic ellipsometry is a nondestructive optical characterization technique that has been used for the analysis of organic materials and device performance.[6,7] It is based on measurement of the polarization of a beam of light reflected from the surface of the sample at a known angle of incidence. Thus no reference samples are needed for calibration. Two parameters (ψ and Δ) are measured as functions of wavelength and the angle of incidence. These parameters are related to the complex reflectivity ratio ρ:

$$\rho = \frac{r_p}{r_s} = \tan\psi \cdot e^{i\Delta}, \tag{1}$$

where r_s and r_p are the complex reflection coefficients for light polarized perpendicular and parallel to the plane of incidence, respectively. A model for the optical structure of the sample is constructed after data are acquired covering the desired spectral range and angles of incidence. The Fresnel equations with the assumed model are then used to predict the expected ψ and Δ data for the wavelength, and angles of incidence chosen. Data fitting is then applied by adjusting the model parameters to find the best-fit values. The Marquardt–Levenberg algorithm is most commonly used to quickly determine the model that exhibits the smallest difference between the measured and calculated values. The difference is quantified by using mean squared error (MSE) as defined by

$$\mathrm{MSE} = \frac{1}{2N-M}\sum_{i-1}^{N}\left[\left(\frac{\tan\psi_i^{\mathrm{Mod}} - \tan\psi_i^{\mathrm{Exp}}}{\sigma_{\psi,i}^{\mathrm{Exp}}}\right)^2 - \left(\frac{\cos\Delta_i^{\mathrm{Mod}} - \cos\Delta_i^{\mathrm{Exp}}}{\sigma_{\Delta,i}^{\mathrm{Exp}}}\right)^2\right], \tag{2}$$

where N is the number of $\psi-\Delta$ pairs, and M is the number of variable parameters used in the model.

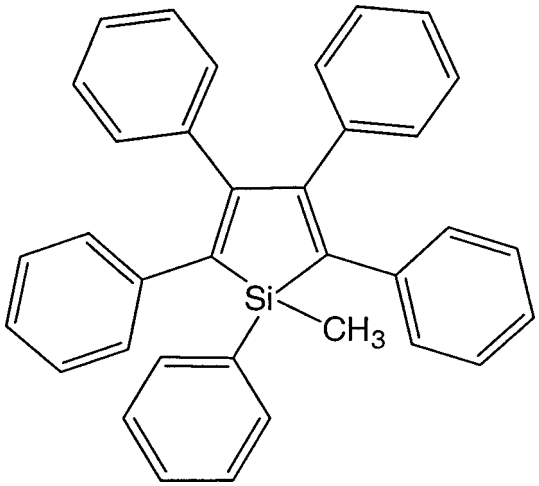

FIG. 1. Structure of the MPS molecule.

III. EXPERIMENTAL PROCEDURE

Figure 1 shows the structure of the MPS molecule. It is a substituted siliole, of which there are several other variations. The organic film layer was deposited on silicon wafer because of the higher reflectance of the substrate and hence higher accuracy in obtaining the reflectance data. The premise is that the optical constants of the MPS film should not depend on whether the substrate is glass or silicon. The silicon substrates were cleaned in 10:1 Piranha solution for 10 min to remove organic contaminants and particles and then dipped in HF solution for oxide stripping. This was then followed by rinsing in DI water and N_2 drying. After cleaning, the substrate was transferred immediately to the vacuum chamber for OLED thin film deposition. Another quartz substrate was prepared at the same time for calibration. The film deposition experiment was performed using Dentor DV502 thermal evaporator. The MPS powder was put in a dimpled sheet-metal tungsten boat, with two substrates placed about 20 cm above. The substrate was rotated during evaporation to enhance the film thickness uniformity. The MPS film was deposited at a rate of 3 Å/s under a base pressure of 2×10^{-6} Torr. The final thickness of the sample, as measured with a quartz crystal monitor, was 1020 Å. The thickness reading from the quartz monitor was calibrated using a surface profiler. The SE measurement was done at room temperature within 3 h after sample preparation. The surface morphology of the samples was also checked by means of an *ex situ* atomic force microscopy (AFM), using a Digital Instruments Nanoscope I. The AFM images were acquired in the repulsive force regime with a force constant of the order of 1 nN between the AFM tip and sample surface.

We used a Jobin–Yvon UVISEL phase-modulated spectroscopic ellipsometer for the SE measurement. The incident angle was set at 70°. The measurement was performed over the spectral range from 250 to 800 nm, with sampling steps of 5 nm. The ellipsometry data was fitted by the commercial software DeltaPsi 1.4 from Jobin–Yvon.

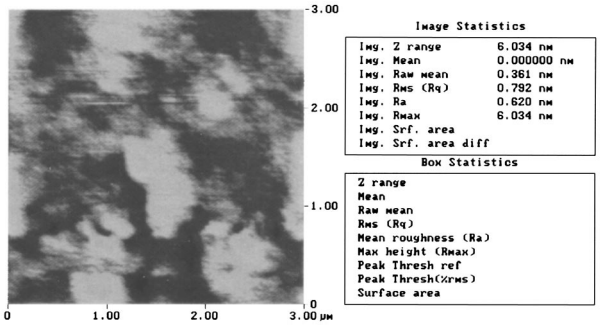

FIG. 2. AFM image of the MPS surface with a size of 3 μm×3 μm showing the rms surface roughness about 8 Å.

IV. MODELING AND DATA FITTING

First, it is important to independently assess surface roughening because the presence of roughness has an impact on the accuracy and precision of film thickness and optical constant measurements. Figure 2 shows the topography of MPS measured by AFM. The rms surface roughness is less than 8 Å. Such small roughness can be ignored in SE modeling without affecting the fitting results. Thus, a four-phase model (ambient/MPS/oxide/Si) was assumed for regression analysis, as shown in Fig. 3. In this model, the optical dispersion of the native oxide layer was described by a dielectric function for a thermal oxide. The optical constants of the Si substrate were obtained from Jellison.[8]

For MPS layer, thickness and all the optical constant related parameters can be set to be fixed or free for fitting. In the following fitting procedure, the adopted model parameters and the thickness of MPS were all freely varied. The MPS layer was assumed to be isotropic, which is reasonable due to its small thickness ($\sim$100 nm) and random orientation of the molecules. Since MPS is transparent in the visible range, Sellmeier dispersion formula was used to represent the optical properties of the thin films. The Sellmeier equations used are

$$n(\lambda)^2 = A + \frac{B\lambda^2}{\lambda^2 - C^2}, \tag{3}$$

$$k(\lambda) = 0, \tag{4}$$

where *A*,*B*, and *C* are fitting parameters and λ is the wavelength of incident light. Using this model, a best fit was obtained in the range of 450 to 800 nm. The best fit thickness

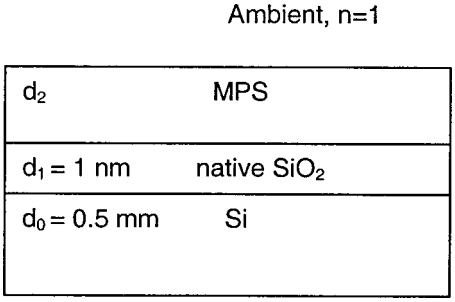

FIG. 3. The four-phase structure model for the MPS sample and the molecular structure of MPS.

TABLE I. Best-fit parameter values resulting from regression analysis of ellipsometric measurements by the Sellmeier model

	A	B	C	Thickness (Å)	MSE
Value	1.836	0.701	269.3	1043.4	6×10^{-5}
Uncertainty	0.082	0.078	9.2	0.2	

of the MPS film was 1043 Å which was very close to the crystal oscillator measurement. All the best-fit parameter values and the uncertainties are list in Table I. The fitted native oxide thickness was 11 Å with an uncertainty of 1 Å. In the following fitting procedures, the native oxide thickness was fixed at this value.

When we extended the fitting range to shorter wavelength, the MSE became much larger. This indicated that the Sellmeier transparent model became insufficient in the range $\lambda<450$ nm, which meant the absorption could not be neglected. This is obvious since there are absorption bands in the blue-uv region. We then tried to use the classical Lorentz oscillator model (LOM) with three oscillators to fit the whole data range. In LOM, the dielectric function is expressed as

$$\varepsilon=(n-ik)^2$$

$$=\varepsilon_\infty+\frac{(\varepsilon_\infty-\varepsilon_s)\omega_0^2}{\omega_0^2-\omega^2+i\gamma_0\omega}+\sum_j^2\frac{f_j\omega_{Tj}^2}{\omega_{Tj}^2-\omega^2+i\gamma_j\omega}, \qquad (5)$$

where ε_∞ is the high frequency contribution to the dielectric constant, ε_s is the static dielectric constant, ω is photon frequency, ω_{tj} is the j_{th} resonant frequency, f_j is the j^{th} oscillator strength, and γ_j is the j^{th} damping constant. Best fitting was obtained with a MSE of 0.001. The best fit parameter values are given in Table II. Figure 4 shows the calculated $\tan(\Psi)$ and $\cos(\Delta)$ values. It can be seen that they agreed well with the experimental data in the whole measurement range except in the range of 350 to 500 nm. A four-ocsillator LOM was attempted but no significant improvement to the fitting was achievable. It is believed to be due to the lack of experimental data in shorter wavelengths. The two resonances obtained in the uv region in Table II are sufficient to describe the data.

As mentioned above, LOM cannot fit the experimental data well in the range of 350 to 500 nm, which is actually near the absorption band gap edge. In this region, we tried to use the amorphous semiconductor model for the dispersion of MPS. This model was developed by Forouhi and Bloomer (FB).[9] It is particularly efficient for semiconductors and amorphous dielectric materials, especially in a small energy range.[10] According to the FB model, n and k can be expressed as function of the transition energy E:

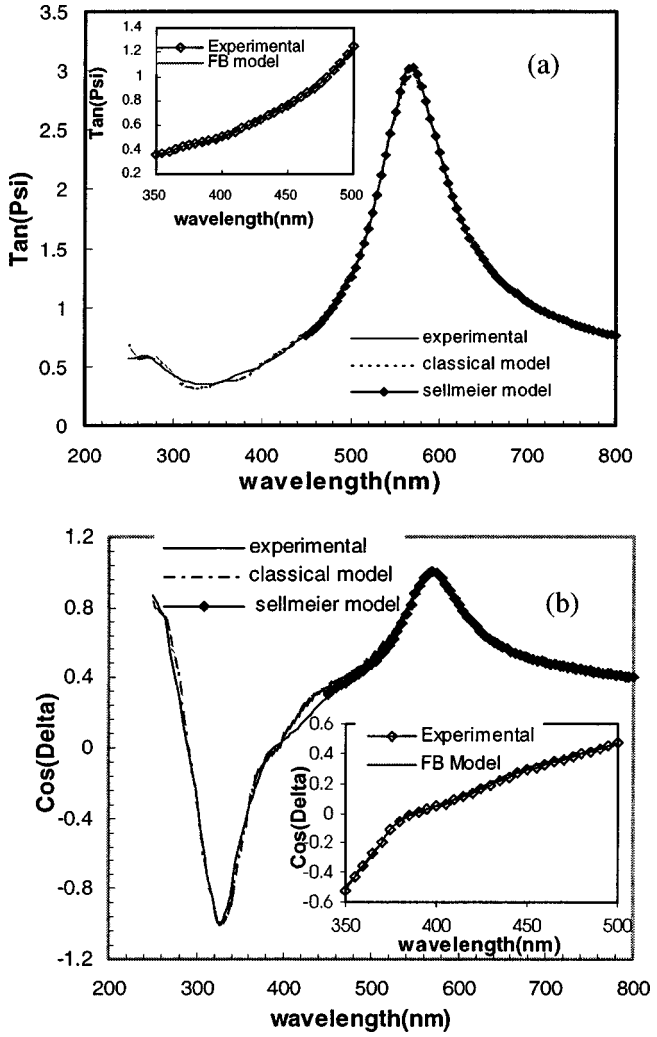

FIG. 4. Experimental data and the best fit curves for (a) $\tan(\psi)$ and (b) $\cos(\Delta)$ at an incidence angle of 70°.

$$n(E)=\sqrt{\varepsilon_\infty}+\frac{B_0E+C_0}{E^2-BE+C}, \qquad (6)$$

$$k(E)=\frac{A}{E^2-BE+C}(E-E_g)^2, \qquad (7)$$

where

$$B_0=\frac{2A}{\sqrt{4C-B^2}}\left(-\frac{B_i^2}{2}+E_gB-E_g+C\right), \qquad (8)$$

$$C_0=\frac{2A}{\sqrt{4C-B^2}}\left[(E_g^2+C)\frac{B_i^2}{2}-2E_gC\right]. \qquad (9)$$

TABLE II. Best-fit parameter values resulting from regression analysis of ellipsometric measurements by the Lorentz oscillator model.

	ε_∞	ε_s	ω_0 (eV)	γ_0 (eV)	f_1	ω_1 (eV)	γ_1 (eV)	f_2	ω_2 (eV)	γ_2 (eV)	Thickness (Å)
Value	1.556	2.353	6.519	0.005	0.035	3.337	0.373	0.144	4.759	0.917	1049.5
Uncertainty	0.132	0.019	0.28	0.089	0.003	0.005	0.021	0.026	0.025	0.080	3.4
MSE	0.001										

TABLE III. Best-fit parameter values resulting from regression analysis of ellipsometric measurements by the FB model.

	ε_∞	A	B	C	E_g (eV)	Thickness (Å)	MSE
Value	2.756	0.041	6.192	9.669	2.779	1045.9	5×10^{-5}
Uncertainty	0.008	0.002	0.020	0.034	0.007	1.3	

In this model, A is related to the position matrix element of electron transition, B is proportional to the transition energy gap, C is related to damping factor of the transition and energy gap, ε_∞ is the asymptotic value of n when E tends to be very large and E_g is the band gap energy. As shown in Fig. 4, the fitting using the FB model agrees very well with the experimental data. The best fit parameters are given in Table III. Note that the thicknesses of the MPS layer obtained by the three models are almost same, which is a necessary condition for the fitting process.

V. RESULTS AND DISCUSSION

The optical properties of OLED materials are essentially dependent on their complex dielectric functions, which are related to the refractive index n and extinction coefficient k. With fitted dispersion models, the n and k of MPS as a function of wavelength from 250 to 800 nm are given in Fig. 4. Note that the n, and k values are calculated using the best fitting models in different wavelength range. One interesting point is the fundamental absorption edge, which manifests itself by a rapid change in absorption, can be used to determine the energy gap of the semiconductor. Figure 5 shows that when the wavelength is less than 450 nm, the k value increases quickly. That indicates the fundamental absorption edge is at about 450 nm, which corresponds to the band gap of the MPS. In fact, one of the fitting parameters of the FB model is the band gap energy. The fitting result is 2.78 eV. We also used cyclic voltammetry (CV) to measure the highest occupied molecular orbital (HOMO) and lowest unoccupied molecular orbital (LUMO) levels of MPS. The measured HOMO and LUMO levels were -3.05 and -5.82 eV, respectively, which gave a band-gap energy of 2.77 eV. This value is very close to that obtained by SE measurement.

Figure 6 shows the absorption coefficient derived from k value according to the well-known relationship

$$\alpha = \frac{4\pi k}{\lambda}, \tag{10}$$

where λ is in cm. Two absorption peaks, as indicated in Fig. 6 are at 368 and 262 nm. We also measured the absorbance of the sample with MPS film deposited on quartz substrate using a spectrophotometer. Two peaks are observed from the absorption spectrum inserted in Fig. 6, at 369 and 252 nm, respectively. The agreement of measuring peaks with the fitting values is very good. Those absorption peaks from the fitting data correspond to transition energies 3.37 and 4.76 eV using the Lorentz model. The associated damping constants are 0.373 and 0.917 eV, respectively. In the Lorentz model, the damping coefficients γ_i are related to the homogeneous broadening linewidths in the absorption spectra by $\Delta\nu = \gamma/2\pi$. The inverse of γ gives the dephasing time of the electronic transition corresponding to the resonance. From Table II, the dephasing times are 1.1×10^{-14} s and 4.5×10^{-15} s, respectively. These are typical numbers for amorphous solids.[11]

In the region near the main absorption peak in the visible, the FB model is more suitable to fit the data. This is in agreement with the fact that MPS is an organic amorphous semiconductor. In amorphous semiconductors, the k selection rule is relaxed due to the disordered structure. In fact, the wave vector k cannot be defined owing to lack of periodic structures. It is assumed that (1) in a limited range of photon energy, the energy dependence of the transition is neglected, that is, the momentum matrix element is constant, and (2) the extended states of the valence and conduction bands whose density of states have a square root dependence on phonon energy. Under these assumption the absorption is believed to take place between extended states and is described as[10]

$$(\alpha E)^{1/2} = B^{1/2}(E - E_g), \tag{11}$$

where B is a proportional constant independent of photon energy and $B^{1/2}$ gives a measure of disorder effect in band edge. Eq. (11) predicts a linear dependence of $(\alpha E)^{1/2}$ on the photon energy. Figure 7 shows the spectral variation of the

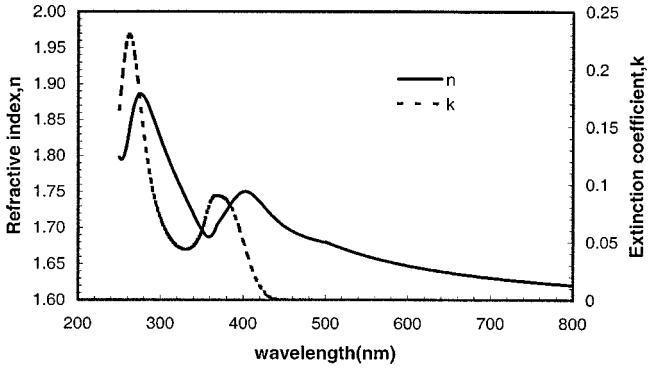

FIG. 5. Refractive index and extinction coefficient of MPS obtained by spectroscopic ellipsometry.

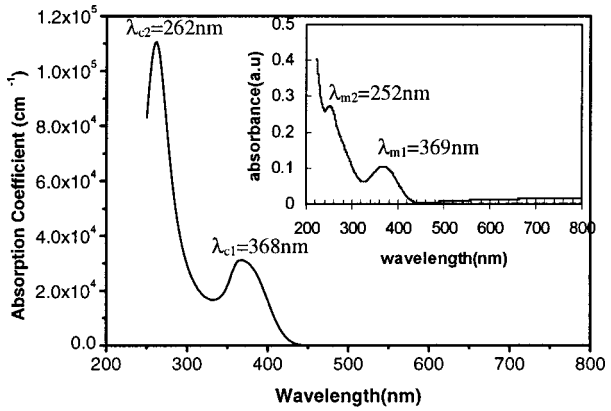

FIG. 6. Comparison between experimental (inset) and fitted absorption spectra.

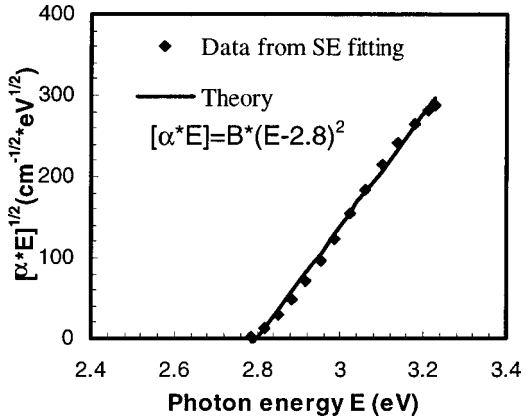

FIG. 7. Fitting of the absorption edge data to the amorphous semiconductors model.

absorption coefficient for MPS as compared to the theoretical predictions. The band gap energy in theoretical model uses the fitting value 2.8 eV. We note that near the band edge, the photon energy is from 2.77 to 3.2 eV in our experiment, the sharp absorption edge is best fitted by the $(E-E_g)^2$ dependence. It is also interesting that the obtained value of B, which is $4.9\times10^5\mathrm{cm}^{-1}\ \mathrm{eV}^{-1}$, is similar to those of many amorphous semiconductors.[12] Those results agree well with the absorption model for amorphous semiconductors.

The external quantum efficiency of an LED is the product of internal quantum efficiency and the photon extraction efficiency. For conventional semiconductor LEDs the extraction efficiency η is calculated simply by integration of the emission intensity [$I(\theta)=$ constant for isotropic dipoles in this case] over surface-extracting cone and divided by the total emission (half-spherical emission).[13] For large n,

$$\eta=1-\cos\theta_c=1-\left(1-\frac{1}{n^2}\right)^{1/2}\approx\frac{1}{2n^2}, \tag{12}$$

where $\theta_c=\sin^{-1}(1/n)$ is the critical angle which is determined by total internal reflection. This extraction efficiency is used to calculate the maximum external quantum efficiency. Blue-green light with a peak wavelength at 490 nm was obtained from the OLED using MPS as emitting material. The SE fitting shows $n(490\,\mathrm{nm})=1.68$. Using the above η relationship and assuming the singlet:triplet branching ratio is 1:3, the maximum external fluorescent quantum efficiency can be calculated to be 4.9%, which is smaller than that measured experimentally.[3] However, the above derivation of η is based on the ray optics. For OLEDs that may not be valid because each layer thickness is usually less than 200 nm, which is much less than emission wavelength. Benisty *et al.* reported that η was $1/n^2$ in a ''close'' mirror configuration considering the interference from the cathode mirror.[4] Recently, Kim *et al.* pointed out the efficiency should be $0.75/n^2$ to $1.2/n^2$, depending on the alignment conditions of emitting dipoles.[5] Using the average figure of $1/n^2$, the maximum n_{QE} of the MPS OLED should be 9%. Thus the external quantum efficiency of 8% obtained in our experiment does not violate the theoretical limit.[3]

VI. SUMMARY

In summary, we have used spectroscopic ellipsometry to investigate the optical properties of intrinsic MPS grown on silicon substrate by thermal evaporation. The SE spectra were modeled by using Sellmeier approximation, Forouhi–Bloomer, and classical Lorentz models in different wavelength ranges. These models provide a good description of the obtained SE spectra. Accurate refractive index and extinction coefficients in a wavelength range from 250 to 800 nm were obtained. The derived absorption spectra agree well with that measured by spectrophotometry. In addition, the energy gap of the material is derived from the FB model with a value that is very close to that obtained by CV measurement. By studying the optical absorption properties near the band gap, it is concluded that the organic material is very similar to amorphous inorganic semiconductors in terms of optical properties.

ACKNOWLEDGMENT

This research was supported by the Hong Kong Research Grants Council, Grant No. HKUST6051/00E.

[1] S. R. Forrest, IEEE J. Sel. Top. Quantum Electron. **6**, 1072 (2000).
[2] G. E. Jabbor, B. Kippelen, N. R. Armstrong, and N. Peyghambarium, Appl. Phys. Lett. **73**, 1185 (1998).
[3] H. Y. Chen, W. Y. Lam, J. D. Luo, Y. L. Ho, B. Z. Tang, D. B. Zhu, M. Wong, and H.S. Kwok, Appl. Phys. Lett. **81**, 574 (2002).
[4] H. Benisty, H. De Neve, and C. Weisbuch, IEEE J. Quantum Electron. **34**, 1612 (1998).
[5] J. S. Kim, P. K. Ho, N. C. Greenham, and R. H. Friend, J. Appl. Phys. **88**, 1073 (2000).
[6] F. G. Celii, T. B. Harton, and O. F. Phillips, J. Electron. Mater. **26**, 366 (1997).
[7] B. Masenelli, S. Cllard, A. Gagnaire, and J. Joseph, Thin Solid Films, **364**, 264 (2000).
[8] G. E. Jellison, Opt. Mater. **1**, 41 (1992).
[9] A. R. Forouhi and I. Bloomer, in *Handbook of Optical Constants of Solids II*, edited by E. Palik (Academic, San Diego, 1991).
[10] K. Morigaki, *Physics of Amorphous Semiconductors* (World Scientific, Singapore, 1999), Chap. 8.
[11] G. L. Huang, Y. J. Xie, and H. S. Kwok, J. Opt. Soc. Am. B **9**, 2019 (1992).
[12] Mott, N. F. and Davis, E. A., *Electronic Processes in Noncrystalline Materials*, 2nd ed. (Clarendon, Oxford, 1979).
[13] B. E. A. Saleh and M. C. Teich, *Fundamental of Photonics* (Wiley, New York, 1991).